AGU ADVANCING EARTH AND SPACE SCIENCES

Geophysical Research Letters

RESEARCH LETTER
10.1029/2026GL122829

Sea Surface Temperature Feedbacks and Convective Organization Mediate the Tropical Circulation Response to Aerosols

Adam B. Sokol[1] and **Chris J. Wright**[2]

[1]Program in Atmospheric and Oceanic Sciences, Princeton University, Princeton, NJ, USA, [2]Department of Atmospheric and Climate Science, University of Washington, Seattle, WA, USA

Key Points:

- Aerosol enhancement in subsiding regions strengthens the large-scale tropical circulation through tighter spatial clustering of convection
- Convective-region aerosol enhancement directly invigorates local convective activity but does not affect large-scale circulation strength
- Sea surface temperature gradient feedbacks drive the large-scale circulation response to aerosols in a fixed mean climate

Supporting Information:

Supporting Information may be found in the online version of this article.

Correspondence to:

A. B. Sokol,
adam.sokol@princeton.edu

Citation:

Sokol, A. B., & Wright, C. J. (2026). Sea surface temperature feedbacks and convective organization mediate the tropical circulation response to aerosols. *Geophysical Research Letters*, *53*, e2026GL122829. https://doi.org/10.1029/2026GL122829

Received 20 MAR 2026
Accepted 28 JUL 2026

Abstract

Coupling between aerosols, atmospheric circulation, and tropical sea surface temperature (SST) patterns is an important part of anthropogenic influence on climate but is not well understood. Using idealized, cloud-resolving simulations with a slab ocean, we examine the hydrologic and circulation responses to uniform and spatially varying aerosol enhancement. The equilibrium responses are decomposed into forcings attributable to aerosol-cloud interactions and feedbacks associated with SST gradient adjustment. Aerosol enhancement within convective regimes forces an increase in deep convective mass flux but has only a modest, feedback-driven impact on large-scale circulation. Enhancement within subsiding regimes does not affect convective mass flux but strengthens the large-scale circulation through direct forcing and SST gradient feedbacks; the forcing component is explained by changes in low-level buoyancy and convective organization. These results highlight the mediating roles of convective organization and SST patterns in aerosol-cloud-circulation coupling on long timescales.

Plain Language Summary

Aerosol particles modify the properties of clouds through their influence on cloud droplet number and size. High aerosol concentrations generally delay the formation of rainfall within clouds and make them more reflective of sunlight, both of which can have downstream impacts on the atmospheric circulation and Earth's energy budget. We use a high-resolution model to study how different patterns of aerosol pollution impact underlying sea surface temperature patterns, the spatial distribution of rainfall, and the strength of small-scale and large-scale atmospheric circulations. We find that aerosol pollution in moist, rainy regions boosts local storm activity but has no immediate effect on the large-scale (thousands of kilometers) circulation. In contrast, pollution in clear, dry regions strengthens the large-scale circulation through a spatial reorganization of storm activity, although the total amount of storm activity is not impacted. In both of these cases, in addition to an experiment with a uniform pollution, cloud and circulation adjustments to pollution drive changes in sea surface temperature contrast between the rainy and dry regions, which have significant secondary impacts on large-scale circulation strength and precipitation.

1. Introduction

By serving as cloud condensation nuclei, aerosol particles brighten liquid clouds by increasing cloud droplet number concentration for a fixed condensate mass (Twomey, 1974). These microphysical changes suppress the formation of rain by droplet collision-coalescence, altering the distribution of latent and radiative heating within clouds, as well as mixing between clouds and their environment (Gunn & Phillips, 1957; Rosenfeld, 1999; Stevens et al., 1998). Collectively, these processes allow aerosols to exert pronounced, albeit uncertain, influence on cloud fraction (Albrecht, 1989; McFarquhar & Wang, 2006), cloud thickness (Bretherton et al., 2007; Pincus & Baker, 1994; Wood, 2007), updraft intensity (Abbott & Cronin, 2021; Igel & van den Heever, 2021; Blossey et al., 2018), and lightning frequency (Thornton et al., 2017; Wright et al., 2025), among other cloud properties. While these cloud adjustments to aerosols have been the focus of a large body of research, their implications for the large-scale atmospheric circulation are not well understood.

Recent work has revealed that aerosol-cloud interactions (ACI) can influence the large-scale tropical circulation via atmospheric stratification and moisture transport (Beydoun & Hoose, 2019; Dagan, 2022, 2024; Dagan & Chemke, 2016; Dagan et al., 2023, 2025; Heever et al., 2011; Hwang et al., 2024; Nishant et al., 2019; Yamaguchi et al., 2026). Using a cloud-resolving model to simulate an overturning circulation analogous to the Pacific Walker circulation, Dagan et al. (2023) found that circulation strength increases in response to enhanced aerosol

10.1029/2026GL122829

number concentration (N_a), specifically when enhancement occurs within the subsiding branch of the circulation. Homogeneous-SST experiments have shown both strengthening and weakening circulation responses (Dagan, 2024; Dagan et al., 2025), underscoring the complexity of modeling aerosol-cloud-circulation coupling. Seeking to understand how this coupling contributes to the effective radiative forcing from ACI, these previous experiments have used fixed sea surface temperature (SST), which is justified by the slow response time of SST compared to the timescale of circulation adjustment. Yet, coupled model experiments suggest that SSTs can adjust to aerosol forcing within a year or two, and that aerosols have shaped the surprising pattern of SST change over recent decades (Deser et al., 2020; Heede & Fedorov, 2021; Hwang et al., 2024; Takahashi & Watanabe, 2016). These experiments demonstrate that SST, convective-scale processes, and large-scale atmospheric circulation are tightly intertwined in the tropics (Emanuel et al., 1994; Lindzen & Nigam, 1987; Pierrehumbert, 1995). Understanding the interplay between ACI, SST patterns, and the tropical circulation is therefore essential for gaining a complete picture of aerosols' influence on climate.

This paper builds on previous work in two ways. First, we investigate how SST-mediated feedbacks influence the equilibrium hydrologic and circulation responses to different spatial patterns of aerosol enhancement. By allowing ACI to reshape the SST gradient, we demonstrate that SST feedbacks generated by cloud-scale processes play an important role in the total circulation response. Second, we examine the circulation response to aerosol at two distinct physical scales: the “cloud scale,” quantified as the convective mass flux and representative of the total convective activity in the tropical troposphere, and the “large scale”, quantified as the time-mean circulation strength and analogous to the climatological Walker circulation in the equatorial Pacific. While these two circulation metrics are closely related—convective updrafts generate the ascent associated with the time-mean circulation—we will show that they respond disparately to aerosol enhancement. The divergent responses are reconciled by changes in the spatial organization of deep convection. We also identify a new mechanism for the direct invigoration of the large-scale circulation by aerosols in the absence of any SST change.

We simulate aerosol-cloud-circulation interactions in a coupled system in which the domain-mean SST is fixed but the local SST can interactively respond to imposed aerosol perturbations. In such a system, the forced response of variable χ to a N_a perturbation can be decomposed into a forcing term ($\Delta_a \chi$) and a feedback term ($\Delta_T \chi$):

$$\Delta\chi \quad = \Delta_a\chi + \Delta_T\chi \tag{1}$$

where T represents the SST state vector (note the difference from traditional climate feedback analysis, in which T would be the mean surface temperature). The forcing term is the forced change in χ under fixed T and includes cloud and circulation adjustments:

$$\Delta_a\chi \quad = \left(\frac{\partial\chi}{\partial N_a}\right)_T \Delta N_a\,. \tag{2}$$

Here, the forcing does *not* include direct aerosol-radiation interactions, as we focus only on ACI. The SST-mediated feedback term is the additional change in $\mathcal{X}$ resulting from the T response to N_a enhancement:

$$\Delta_T\chi = \left(\frac{\partial\chi}{\partial T}\right)_{N_a} \left(\frac{\partial T}{\partial N_a}\right)\Delta N_a. \tag{3}$$

2. Model Simulations

Idealized simulations are conducted using the System for Atmospheric Modeling (SAM; Khairoutdinov & Randall, 2003) with the two-moment M2005 microphysics scheme (Morrison et al., 2005). The model domain is $3{,}072 \times 256\ \text{km}^2$ with 2-km horizontal resolution, walled boundaries in the x direction, and periodic boundaries in the narrow y direction. Insolation is constant in space and time following the RCEMIP protocol (Wing et al., 2018). Complete model specifications are provided in Text S1 in Supporting Information S1.

To model the SST feedbacks associated with aerosol enhancement, we couple the atmospheric model to a modified slab ocean that maintains constant $\overline{\text{SST}}$ but allows the local SST to vary over time. Simulations are initialized with $\mathrm{SST}(x,y,t=0)=\overline{\mathrm{SST}}-\delta\mathrm{SST}\cos(\pi x/L)$ where $\overline{\mathrm{SST}}=300$ K is the mean and $\delta\mathrm{SST}=1$ K. This pattern is fixed for 30 days of spin-up time, after which the slab ocean is enabled. The local SST varies in response to the spatially anomalous surface energy imbalance:

$$c\frac{\partial}{\partial t}\mathrm{SST}(x,y,t)=Q(x,y,t)-\overline{Q}(t). \quad (4)$$

where Q is the net heat flux into the slab and c the slab heat capacity, which corresponds to a depth of 10 m. Q includes radiative, latent, and sensible heat fluxes, plus a temporally fixed ocean heat source Q_{ocn} with the same spatial structure as the initial SST and a 70 W/m^2 difference between its minimum and maximum (Text S1 in Supporting Information S1). This simple representation of ocean energy transport is used here to maintain a zonal SST gradient, as is typical in mock-Walker experiments (e.g., Bretherton, 2007; Peters & Bretherton, 2005). Our choice to maintain fixed $\overline{\mathrm{SST}}$ was due to practical considerations: a test run with fully interactive SST did not equilibrate to the imposed N_a perturbation after 800 days, and the $\overline{\mathrm{SST}}$ cooling was so large that the model entered a markedly different climate state.

In the M2005 microphysics scheme, cloud condensation nuclei (CCN) are activated within updrafts according to the power-law function $\mathrm{CCN}=N_aS^k$, with no explicit representation of aerosol type or size. S is the supersaturation, N_a the CCN concentration at 1% supersaturation, and k a constant set to 0.4 for typical oceanic conditions (Twomey, 1959). Following previous work (Dagan, 2024; Dagan et al., 2023, 2025), we impose aerosol perturbations by varying N_a between values characteristic of clean conditions (20 cm^{-3}) and of highly polluted conditions (2,000 cm^{-3}). The imposed changes in N_a do not impact radiation directly, but do so indirectly through their impact on cloud droplet number and size.

In the control simulations, which we call *clean*, we set $N_a=20$ cm^{-3} uniformly. We then test three different aerosol pollution patterns, shown in Figure 1c, in which N_a is a specified function of x and there is no aerosol advection. In pollUNI, we set $N_a=2000$ cm^{-3} across the entire domain. In *pollCON* and *pollSUB*, we impose polluted conditions only over the warm, convective half and cool, subsiding half of the domain, respectively, maintaining clean conditions in the unperturbed half. The analytical specifications for $N_a(x)$ are given in Text S2 in Supporting Information S1, and the resulting microphysical adjustments are shown in Figure S1 in Supporting Information S1.

2.1. Forcing-Feedback Framework

We conduct 400-day, interactive-SST simulations for each of the four N_a patterns. The equilibrium $\Delta\chi$ relative to clean conditions represents the total forced response to the N_a perturbation. To separate the forcing and feedback, we conduct four fixed-SST simulations that are branched from day 300 of the clean, interactive-SST run and all adopt the same instantaneous SST pattern from that point. The pattern is less smooth than the time-averaged SST fields but is similar in structure (Figure 1d). The fixed-SST runs are integrated for 250 days, and for all simulations, the last 200 days are used for analysis. The change in χ relative to clean conditions in the fixed-SST runs is taken as the forcing $\Delta_a\chi$, and the feedback is then $\Delta_T\chi=\Delta\chi-\Delta_a\chi$. The SST pattern adopted in the fixed-SST simulations is a potential source of uncertainty in our results, as $\Delta_a\chi$ could plausibly be sensitive to SST gradient strength.

3. Results

This section begins with a discussion of the SST gradient response to N_a perturbations in the coupled experiments. We then discuss changes in convective organization and the hydrologic cycle before turning to the tropical circulation response. We focus on two interrelated but distinct measures of circulation strength, the convective mass flux and the time-mean circulation mass flux, both of which are critical for understanding tropical climate.

3.1. SST Response to Aerosol Enhancement

We first examine the SST response to aerosol enhancement in the coupled simulations. Because the slab ocean model maintains fixed mean temperature, local SST responds only to the spatially anomalous part of the surface energy flux imbalance.

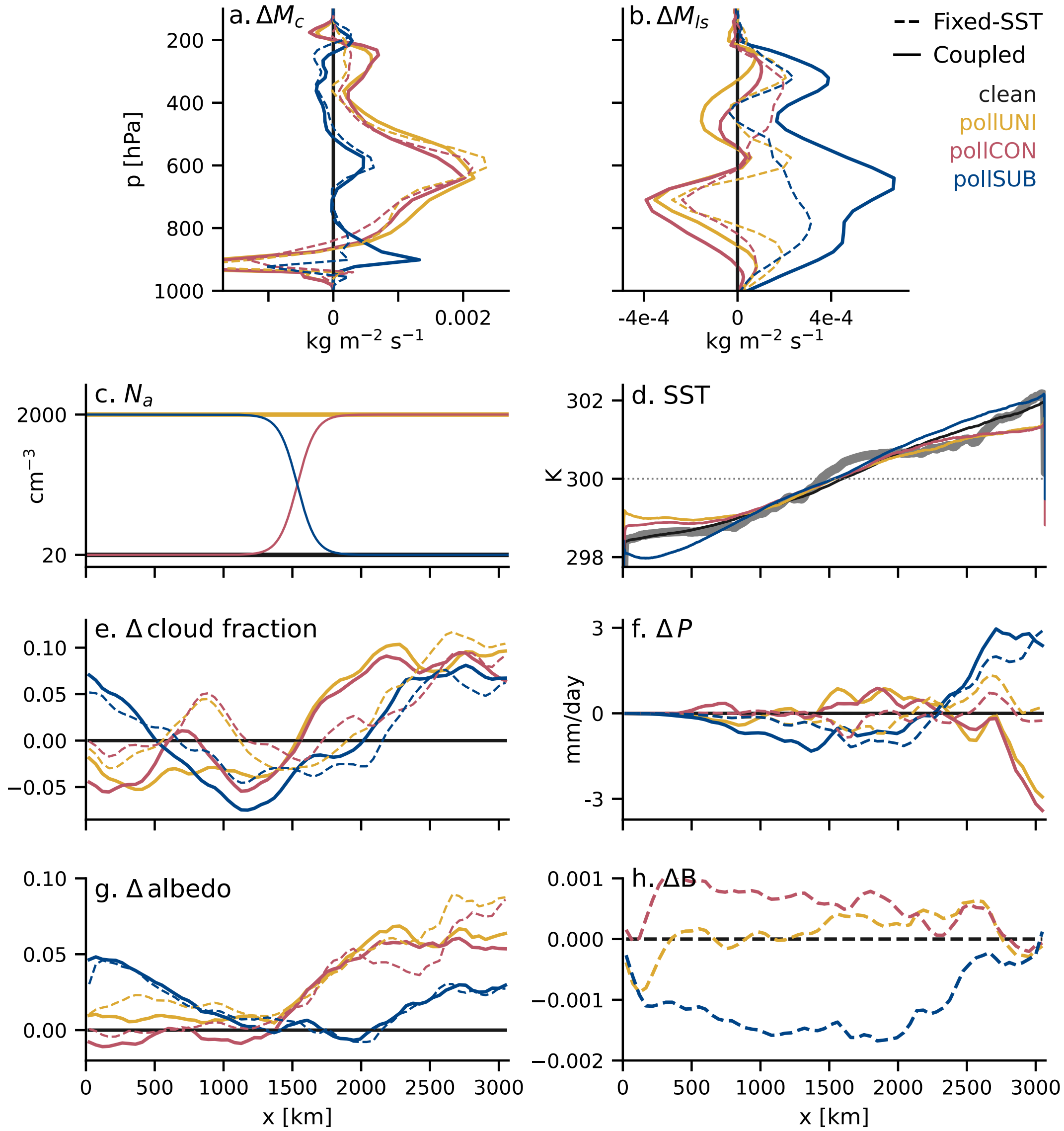

Figure 1. Results from the coupled (solid) and fixed-SST (dashed) simulations. All changes are relative to clean conditions. Change in (a) convective mass flux and (b) large-scale circulation mass flux. (c) Aerosol number concentration. (d) SST in the coupled (thin lines) and fixed-SST simulations (thick gray line). Change in (e) cloud fraction, (f) precipitation P, (g) albedo, and (h) the sub-cloud buoyancy metric B. In (h), only fixed-SST runs are shown to illustrate the forcing mechanism. In (c–h), data are averaged into 48 km chunks for readability.

Figure 1d shows that spatially varying N_a enhancement drives local SST cooling in the polluted region, which must be offset by warming in the unpolluted region in order to maintain constant $\overline{\mathrm{SST}}$. In pollCON, this response arises from a large brightening of the convective region (Figure 1g), which shades the warm-pool surface and weakens the zonal SST gradient. The local albedo increase can be attributed both to cloud brightening via microphysical adjustments and to an increase in cloud fraction (Figure 1e), that is, to both the first and second aerosol indirect effects (Albrecht, 1989; Twomey, 1974).

In pollSUB, subsiding-region albedo enhancement leads to an increase in SST gradient. As discussed in the next section, convective precipitation and clouds become increasingly concentrated over the warmest SSTs (Figures 1e and 1f), leading to remote albedo enhancement in the unperturbed convective region. Thus, as has been suggested before (Dagan, 2022), subsiding-region N_a enhancement has both local and remote brightening effects, with the latter associated with changes in convective organization.

Surprisingly, the response to spatially uniform N_a enhancement (pollUNI) very closely resembles the response to convective-region enhancement, with marked brightening of the convective region and SST gradient weakening. That the pollUNI response so closely resembles the pollCON response suggests that uniform N_a enhancement preferentially brightens the convective region, which is consistent with the greater baseline cloudiness there relative to the subsiding region (not shown).

For all N_a patterns, there is temporal variability in SST gradient strength (Figure S8 in Supporting Information S1), as has been shown previously in idealized, cloud-resolving simulations (Sokol et al., 2025). The impact of SST gradient variability on convection is evident in Hovmöller diagrams of column-integrated water vapor (Figures S10–11 in Supporting Information S1), which show that moist-region size varies considerably in the coupled simulations relative to the fixed-SST simulations. Even in the context of this variability, the changes in time-mean SST gradient are substantial (statistically significant at the 95% level) and may be expected to drive hydrologic and circulation feedbacks. As we show in the following sections, these feedbacks make significant and, in some cases, dominant contributions to the total forced response to aerosol enhancement.

3.2. Changes in Deep Convective Organization

Previous work has shown that both N_a enhancement (Beydoun & Hoose, 2019) and SST gradients (Bretherton & Sobel, 2002; Lindzen & Nigam, 1987) can influence the spatial organization of convection. We quantify organization using an index, L_{org}, that is sensitive to convective clustering at all length scales up to that of the model domain. L_{org}, developed by Biagioli and Tompkins (2023) and described further in Text S3 in Supporting Information S1, is positive in our simulations (Table S1 in Supporting Information S1), indicating that convection is clustered relative to what would be expected from a random Poisson process.

In response to uniform and convective-region N_a enhancement, L_{org} decreases slightly, indicating reduced convective clustering (Figure 2b). The total ΔL_{org} is dominated by a feedback ($\Delta_T L_{org}$) of −3%–4%, which overwhelms the small positive forcing ($\Delta_a L_{org}$) in pollUNI and near-zero forcing in pollCON. The decrease in organization, while not statistically significant at the 95% level, can also be deduced from changes in precipitation and cloudiness in the coupled experiments (Figures 1e and 1f and Figure S9 in Supporting Information S1), which indicate a shift in convective activity from the warmest SSTs toward the center of the domain. These changes are consistent with the weakening of the SST gradient, as previous work has shown that weaker SST gradients are associated with the spreading out of convective activity over a larger region (Bretherton & Sobel, 2002).

Subsiding-region N_a enhancement in pollSUB leads to a statistically significant 16% increase in L_{org} consisting of roughly equal forcing and feedback components. The positive forcing indicates a substantial increase in organization due to remote N_a enhancement in the subsiding region; in Section 3.5, we discuss possible mechanisms for this forced response and show that it is associated with strengthening of the large-scale overturning circulation. The positive feedback is consistent with the strengthening of the SST gradient (Figure 1d), which is expected to lead to a contraction of the convective region (Bretherton & Sobel, 2002). The increase in organization in both the fixed-SST and coupled pollSUB experiments is evident as a shift in precipitation and cloudiness from the convective-region margin to the warmest SSTs (Figures 1e and 1f, Figure S4 in Supporting Information S1).

The organization changes discussed here have implications for the hydrologic and circulation responses to N_a enhancement, which we discuss below. The magnitude and sign of organization changes are known to be sensitive to the choice of organization index (Mandorli & Stubenrauch, 2024). Nevertheless, the changes in L_{org} found here are qualitatively aligned with the changes in cloudiness and precipitation shown in Figure 1, and with other results shown below. We therefore consider ΔL_{org} to be an adequate metric for understanding the general role of convective organization in the response to aerosol forcing.

3.3. Hydrologic Response to Aerosol Enhancement

Aerosol enhancement impacts both the spatial distribution of rainfall and the domain-mean precipitation $\overline{P}$. Conservation of dry static energy requires $\Delta\overline{P}$ to balance changes in net radiative cooling and sensible heating of the atmosphere (Pendergrass & Hartmann, 2014). We focus on radiative cooling here, as sensible heating changes are very small in comparison. The forcing component of $\Delta\overline{P}$ can arise from changes in cloudiness and moisture, which influence radiative cooling even under fixed SSTs. The feedback component arises primarily from changes

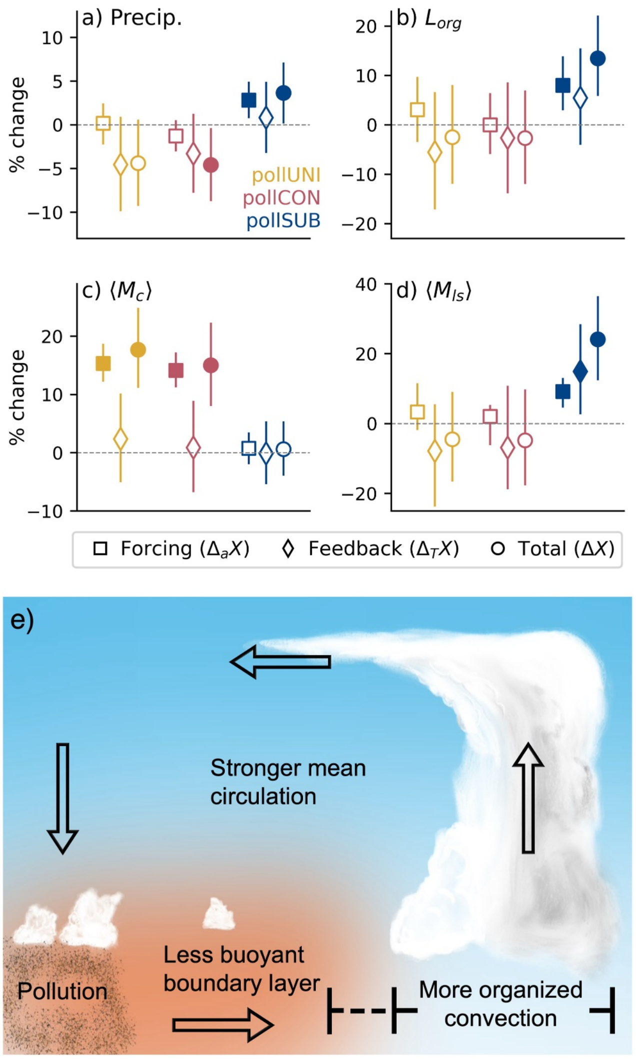

Figure 2. Forcing (squares), feedback (diamond), and total change (circle) in (a) mean precipitation, (b) $\langle M_c \rangle$, (c) $\langle M_{ls} \rangle$, and (d) the convective organization index L_{org}. Error bars show 95% confidence intervals, and solid markers indicate statistically significant responses (see Text S5 in Supporting Information S1). Angled brackets denote the mass-weighted integral between 150 and 800 hPa ($\langle M_c \rangle$) or 150 hPa and the surface ($\langle M_{ls} \rangle$). (e) Schematic showing the system response to subsiding-region N_a enhancement.

in warm-pool SST, which generally control the thermodynamic state of the entire tropical troposphere via deep convection and gravity waves (Emanuel et al., 1994; Sobel et al., 2001).

For the uniform and convective-region pollution cases, $\Delta\overline{P}$ is dominated by the feedback component (Figure 2a). The forcing term is near zero in pollUNI and -1% in pollCON (Figure 2a), with the negative sign of the forcing owing to enhanced convective-region cloudiness, which inhibits longwave radiative cooling. For the feedback, weakening of the SST gradient drives 4.6% and 3.3% reductions in $\overline{P}$ in pollUNI and pollCON, respectively. These reductions are larger than would be expected from the ~0.5 K reduction in warm-pool SST, which, based on a tropical hydrologic sensitivity of 3%/K (He et al., 2024), might be expected to produce a ~1.5% reduction in $\overline{P}$. The additional reduction may be due to reduced convective organization in response to SST gradient weakening, as less organized convection is generally associated with more humid conditions and suppressed radiative cooling in nonconvective regions (Bretherton et al., 2005; Wing et al., 2017).

In pollSUB, $\Delta\overline{P}$ is instead dominated by the forcing term, which accounts for a 2.8% increase in $\overline{P}$, in line with a 2.5 W/m^2 increase in atmospheric radiative cooling (Figure S4 in Supporting Information S1). The radiative cooling increase is almost entirely driven by clear-sky effects, consistent with the increase in convective organization, which allows for more effective radiative cooling in subsiding regimes. SST-mediated feedbacks provide an additional 0.8% increase in $\overline{P}$ in pollSUB, consistent with the ~0.3 K increase in warm-pool SST.

3.4. Convective Mass Flux Response

Turning to aerosol-driven changes in the tropical circulation, we examine the impact of N_a enhancement on the convective mass flux $M_c = \rho\sigma_c w_c$, where ρ is air density, σ_c is the fraction of the domain occupied by cloudy updrafts, and w_c is the mean vertical velocity within cloudy updrafts (A. I. L. Williams & Jeevanjee, 2025). Intuitively, M_c can be thought of as the cloud-scale circulation strength reflecting the frequency and intensity of convective updrafts, which has important implications for high cloud cover (Bony et al., 2016; Jeevanjee, 2022). Our focus is on free-tropospheric M_c associated with deep convection, rather than the contribution from shallow convection in the subsiding region, which is limited to 850 hPa. Cloudy grid cells are identified as those with cloud condensate mixing ratios exceeding 10^{-5} kg/kg (Wing et al., 2020).

We find that changes in M_c are almost entirely due to forcing, with SST-mediated feedbacks not playing a major role (Figures 1a and 2c). Convective-region N_a enhancement forces an increase in free-tropospheric M_c regardless of subsiding-region aerosol conditions; that is, $\Delta_a M_c > 0$ in pollCON and pollUNI. The forcing amounts to a ~14%–15% increase in the mean value of M_c in the free troposphere (150–800 hPa). Because changes in M_c can arise from changes in w_c and/or σ_c, the positive forcing does not necessarily imply stronger updraft speeds within convection, as has been suggested previously (e.g., Fan et al., 2018; Igel & van den Heever, 2021). We find that $\Delta_a w_c$ and $\Delta_a \sigma_c$ both vary substantially with height in pollUNI and pollCON, but it is $\Delta_a \sigma_c$ alone that explains the large $\Delta_a M_c$ at 600 hPa (Figure S3 in Supporting Information S1).

The forced increase in M_c in response to convective-region N_a enhancement can be explained by basic energetic constraints and previously identified ACI mechanisms. As described in Section 3.2, changes in mean precipitation are small (~1% or less) in the fixed-SST pollUNI and pollCON experiments due to constraints from the atmospheric dry static energy budget. By suppressing droplet collision-coalescence, N_a enhancement delays warm rain formation and reduces the precipitation efficiency of convection. Defining the precipitation efficiency as in Li et al. (2022), we find that it decreases by ∼25%–30% due to N_a forcing in the fixed-SST pollUNI and pollCON experiments (Table S1 in Supporting Information S1). This large decrease implies that more convection is required to meet the roughly fixed demand for precipitation.

In contrast to convective-region pollution, subsiding-region N_a enhancement only has a small impact on convective mass flux ($\Delta M_c \approx 0$) resulting from compensation between modest decreases and increases in w_c and σ_c, respectively (Figure S3 in Supporting Information S1).

The M_c response to aerosol perturbation is not significantly impacted by SST feedbacks; that is, $\Delta_T M_c \approx 0$ (Figures 1a and 2c). The physical interpretation is that the ∼0.5 K adjustments to warm-pool SST in the coupled experiments have a small impact on convective dynamics compared to the 100-fold increase in N_a. Thermodynamic arguments have long supported an inverse relationship between surface temperature and convective mass flux (Held & Soden, 2006; Jeevanjee, 2022), with recent work suggesting that M_c at a fixed temperature level decreases by 3%–5% per degree surface warming (A. I. L. Williams & Jeevanjee, 2025). Based on this sensitivity, the warm-pool SST changes in the coupled experiments would be expected to produce a positive feedback of 1%–2% in pollUNI and pollCON—an order of magnitude smaller than the ∼15% forcing. The simulated feedbacks of 2.4% and 0.9% in pollUNI and pollCON, respectively, are close to these predicted values. The warm-pool SST changes in pollSUB are even smaller and therefore $\Delta_a M_c$ is close to zero in that experiment.

3.5. Large-Scale Circulation Response

We now turn to the mass flux associated with the time-mean, large-scale circulation, which we define as $M_{ls} = \rho \sigma_{ls} w_{ls}$, where σ_{ls} is the fraction of the domain with time-mean ascent, and w_{ls} is the time-mean vertical velocity within that ascent region. We compute σ_{ls} from meridional-mean, 3D vertical velocity output that is coarsened in the zonal direction into 48 km chunks. We view the large-scale circulation as analogous to the Pacific Walker circulation, and changes in M_{ls} are conceptually similar to changes in a mass stream function. M_{ls} is shaped not only by M_c, but also by the spatial organization of convection and the location and intensity of downdrafts.

Changes in large-scale circulation strength differ substantially from those in convective mass flux. Uniform and convective-region N_a enhancement drive large-scale circulation weakening, with a 5% reduction in tropospheric-mean M_{ls} in the coupled pollUNI and pollCON runs. The total response arises from a small, forced invigoration of 2%–3% that is overwhelmed by a strongly negative feedback (Figure 2d). The negative feedback is consistent with the simulated weakening of the zonal SST gradient, as SST contrast is known to play a leading-order role in the magnitude and spatial structure of low-level tropical convergence (Hartmann & Michelsen, 1993; Lindzen & Nigam, 1987). Notably, this is the only response examined here in which the sign of the total response differs from the sign of the forcing.

The modest, 2%–3% forcing of M_{ls} in pollUNI and pollCON is notably smaller than the ∼15% forcing of M_c in the same experiments. Such a mismatch implies that most of the increase in convective mass flux is balanced by a local increase in downdraft mass flux within the region of mean ascent. In fact, most of the downdraft increase occurs within clouds (Figure S5 in Supporting Information S1), meaning that enhanced N_a is associated with greater turbulence within deep convective clouds but only a small change in the net upward in-cloud mass transport.

In the recent RCEMIP-ACI model intercomparison project (Dagan et al., 2025), the multimodel ensemble generally predicted a weakening of the tropical circulation at 500 hPa with uniformly increasing N_a. While the strengthened M_{ls} in our fixed-SST pollUNI simulation is within the RCEMIP-ACI intermodel spread, the complex vertical structure of $\Delta_a M_{ls}$ (dashed lines in Figure 1b) suggests that sampling a single vertical level does not adequately characterize the circulation response.

In contrast to uniform or convective-region pollution, subsiding-region pollution leads to marked invigoration of the large-scale circulation, with the forcing and feedback both contributing. There is a 24% increase in tropospheric-mean M_{ls} in the coupled pollSUB experiment, ∼40% of which is attributable to the forcing component and ∼60% to the positive feedback (Figure 2d). The positive sign of the feedbacks reflects the expected strengthening of large-scale circulation in response to a steeper SST gradient (Hartmann & Michelsen, 1993; Lindzen & Nigam, 1987).

We have shown so far in this section that the large-scale circulation response to N_a differs entirely from changes in convective mass flux, and that it can be strongly affected by SST gradient feedbacks. The feedback term is larger than the directly forced M_{ls} adjustment in all three cases, and in some cases flips the sign of the total response. Our results support the previous association of subsiding-region aerosol with forced circulation strengthening (Dagan et al., 2023). In the remainder of this section, we provide a new explanation for this circulation forcing.

3.5.1. Mechanisms of Large-Scale Circulation Forcing by Subsiding-Region Aerosol

Why do subsiding-region aerosol strengthen the large-scale circulation even in the absence of SST feedbacks? The forced increase in M_{ls} in pollSUB results not from an increase in convective activity (as $\Delta_a M_c \approx 0$) but from the spatial reorganization of convective updrafts. Changes in σ_{ls} and w_{ls} show that the region of mean ascent shrinks in area but dynamically intensifies ($\Delta_a \sigma_{ls} < 0$ and $\Delta_a w_{ls} > 0$, respectively), reflecting the increased concentration of convective updrafts in the core of the convective regions at the expense of its margins. This is consistent with the increase in L_{org} (Section 3.2) and the spatial patterns of changes in precipitation (Figures 1f, Figure S4 in Supporting Information S1) and vertical velocity (Figure S2d in Supporting Information S1). A suitable mechanism of circulation forcing must explain these spatial shifts in convective activity.

Dagan et al. (2023) proposed a mechanism of circulation forcing in which subsiding-region aerosols suppress local precipitation from shallow convection, allowing more moisture to be transported by the low-level flow to the convective region, where its eventual diabatic heat release strengthens the circulation. The strengthening is amplified by a wind-induced increase in surface evaporation, which leads to even greater moisture convergence. Indeed, the forced M_{ls} increase in pollSUB is accompanied by greater surface evaporation (Figure S2b in Supporting Information S1), which balances the increase in domain-mean precipitation (Figure 2a) and supports greater moisture convergence in the convective region. However, we can attribute the increase in moisture convergence almost entirely to circulation change itself, with changes in atmospheric humidity playing a minor role (Text S6, Figures S2a, and S2b in Supporting Information S1). The intensification of moisture transport is therefore likely a consequence, not a cause, of circulation strengthening. Further, if the circulation change were driven by changes in diabatic heating and surface enthalpy flux feedbacks, the forced invigoration would occur within convective updrafts, and we would expect to see enhanced M_c. Yet, M_c is unchanged in pollSUB (Figure 2c).

We instead hypothesize that subsiding-region aerosol strengthen the large-scale circulation not through their impact on moisture advection, but through changes in the convective instability of the boundary layer. Previous work suggests that N_a enhancement in subsidence regimes can dry the boundary layer through various mechanisms (Chun et al., 2023; Seifert et al., 2015; Stevens et al., 1998). For example, Seifert et al. (2015) found that aerosol-driven precipitation suppression in trade cumulus regimes deepens the cloud layer, distributing boundary layer moisture across a larger volume and reducing relative humidity (RH). In pollSUB, we find similar changes in RH consistent with deepening of the cloud layer (Figure S7 in Supporting Information S1). The drier boundary layer, which is less favorable for convective instability, is advected by the mean flow from the subsiding region to the margins of the unpolluted convective region, where it effectively reduces the area with favorable conditions for convection. In other words, air within the subsiding-region boundary must travel farther into the warm region before convection becomes energetically favorable.

To quantify changes in convective instability, we compute a low-level buoyancy metric B (Text S4 in Supporting Information S1; I. N. Williams & Pierrehumbert, 2017). Decreases in B in response to a perturbation indicate a local reduction in convective instability. We find that N_a enhancement drives a decrease in B locally within the subsiding region and remotely in the margins of the convective region (Figure 1h), with the largest reductions coinciding with the largest decreases in precipitation (Figure 1f). Changes in B are much smaller over the warmest SSTs but are still slightly negative, reflecting free-tropospheric warming that is known to accompany enhanced convective clustering (Becker et al., 2018; Held et al., 1993; Sokol & Hartmann, 2022; Wing et al., 2017).

4. Discussion

We have examined how aerosol-cloud interactions and resulting SST-mediated feedbacks shape the hydrologic and circulation responses to N_a perturbations in a cloud-resolving model with a slab ocean. The central finding is a notable divergence between changes in convective mass flux and large-scale circulation strength. Convective-region N_a enhancement forces a ~15% increase in upward convective mass flux, but this does not impact large-scale circulation strength due to a local, compensating increase in in-cloud downdrafts. In contrast, subsiding-region N_a enhancement does not impact convective mass flux but invigorates the large-scale circulation by ~24% via both forcing and SST gradient feedbacks. The feedbacks govern the sign and magnitude of the large-scale circulation response in all experiments, amplifying the forced invigoration in pollSUB and weakening the circulation in pollUNI and pollCON.

While our results support the finding by Dagan et al. (2023) that subsiding-region pollution invigorates the large-scale circulation independent of the SST response, we are unable to explain the circulation forcing with their proposed mechanism. We instead hypothesize that subsiding-region aerosol strengthen the large-scale circulation by drying the boundary layer and reducing low-level buoyancy at the convective-region margins. This leads to more concentrated ascent, consistent with changes in a metric of convective organization. The fact that convective organization mediates aerosol-cloud-circulation interactions, together with the large intermodel spread in convective organization in cloud-resolving models (Wing et al., 2020), may explain the range of circulation responses to increased N_a in a recent model intercomparison project (Dagan et al., 2025).

The hydrologic response to aerosol perturbations is similarly shaped by convective organization and SST feedbacks. In the uniform and convective-region pollution cases, SST gradient weakening—driven by enhanced convective-region albedo—and the subsequent expansion of the convective region results in a mean precipitation increase of 3%–5%. In pollSUB, by contrast, contraction of the convective region enhances clear-sky radiative cooling, directly forcing a ~3% precipitation increase that is further intensified by a positive feedback resulting from SST gradient strengthening.

These idealized modeling results may be particularly relevant to quasi-steady aerosol perturbation patterns, such has those introduced by biomass burning (Daniau et al., 2012) or deliberate marine cloud brightening (MCB; Latham, 1990). Proposed MCB interventions involve persistent aerosol injections into subtropical stratocumulus desks found in regions of climatologically subsidence. Our findings suggest that such patterns of aerosol enhancement could impact large-scale circulation strength and the organization of convection in dynamically linked ascent regions. Experiments with a coupled general circulation model have already demonstrated how MCB in the eastern subtropical Pacific could invigorate the Pacific Walker circulation through SST-related and coupled ocean-atmosphere dynamical feedbacks (Xing et al., 2025). Our study underscores the need to better understand the physical mechanisms controlling the remote dynamic response to boundary layer aerosol.

More broadly, our results are relevant to understanding circulation changes driven by aerosol trends and shifting SST patterns in the real world. Observed SST trends over recent decades have been linked, in part, to aerosol forcing and trends in regional aerosol emissions (Deser et al., 2020; Hwang et al., 2024; Takahashi & Watanabe, 2016). Our results reinforce the view that the SST pattern response to ACI is not just a consequence of aerosol perturbations but an active mediator of the circulation and hydrologic responses. Future work should focus on how feedbacks associated with SST pattern change contribute to aerosol radiative effects.

Several limitations of this work should be acknowledged. First, our simulations neglect feedbacks associated with direct aerosol-radiation interactions, mean SST change, and ocean dynamical mechanisms. Second, our model does not realistically simulate the stratocumulus decks typical of subsidence regimes over subtropical oceans; the simulation of different low cloud types would likely result in different degrees of aerosol-driven brightening and local SST cooling. Finally, cloud-resolving models are known to produce varying degrees of convective organization (Wing et al., 2020). It is plausible that different organization states have different susceptibilities to aerosol perturbations.

Conflict of Interest

The authors declare no conflicts of interest relevant to this study.

Availability Statement

Code and model output for this study are available from Sokol and Wright (2026). SAM is available from http://rossby.msrc.sunysb.edu/SAM.html.

Acknowledgments

We thank Guy Dagan and one anonymous reviewer for their helpful feedback. We are grateful for Peter Blossey's guidance and modeling expertise. ABS is supported by award NA23OAR4320198 from the National Oceanic and Atmospheric Administration, U.S. Department of Commerce. The statements, findings, conclusions, and recommendations are those of the authors and do not necessarily reflect the views of the National Oceanic and Atmospheric Administration or the U.S. Department of Commerce. CJW is supported by NSF award AGS-2113494.

References

Abbott, T. H., & Cronin, T. W. (2021). Aerosol invigoration of atmospheric convection through increases in humidity. *Science*, *371*(6524), 83–85. https://doi.org/10.1126/science.abc5181

Albrecht, B. A. (1989). Aerosols, cloud microphysics, and fractional cloudiness. *Science*, *245*(4923), 1227–1230. https://doi.org/10.1126/science.245.4923.1227

Becker, T., Bretherton, C. S., Hohenegger, C., & Stevens, B. (2018). Estimating bulk entrainment with unaggregated and aggregated convection. *Geophysical Research Letters*, *45*(1), 455–462. https://doi.org/10.1002/2017GL076640

Beydoun, H., & Hoose, C. (2019). Aerosol-cloud-precipitation interactions in the context of convective self-aggregation. *Journal of Advances in Modeling Earth Systems*, *11*(4), 1066–1087. https://doi.org/10.1029/2018MS001523

Biagioli, G., & Tompkins, A. M. (2023). Measuring convective organization. *Journal of the Atmospheric Sciences*, *80*(12), 2769–2789. https://doi.org/10.1175/JAS-D-23-0103.1

Blossey, P. N., Bretherton, C. S., Thornton, J. A., & Virts, K. S. (2018). Locally enhanced aerosols over a shipping Lane produce convective invigoration but weak overall indirect effects in cloud-resolving simulations. *Geophysical Research Letters*, *45*(17), 9305–9313. https://doi.org/10.1029/2018GL078682

Bony, S., Stevens, B., Coppin, D., Becker, T., Reed, K. A., Voigt, A., & Medeiros, B. (2016). Thermodynamic control of anvil cloud amount. *Proceedings of the National Academy of Sciences*, *113*(32), 8927–8932. https://doi.org/10.1073/pnas.1601472113

Bretherton, C. S. (2007). Challenges in numerical modeling of tropical circulations. In *The global circulation of the Atmo-sphere* (pp. 302–330). Princeton University Press.

Bretherton, C. S., Blossey, P. N., & Khairoutdinov, M. (2005). An energy-balance analysis of deep convective self-aggregation above uniform SST. *Journal of the Atmospheric Sciences*, *62*(12), 4273–4292. https://doi.org/10.1175/JAS3614.1

Bretherton, C. S., Blossey, P. N., & Uchida, J. (2007). Cloud droplet sedimentation, entrainment efficiency, and subtropical stratocumulus albedo. *Geophysical Research Letters*, *34*(3). https://doi.org/10.1029/2006GL027648

Bretherton, C. S., & Sobel, A. H. (2002). A simple model of a convectively coupled walker circulation using the weak temperature gradient approximation. *Journal of Climate*, *15*(20), 2907–2920. https://doi.org/10.1175/1520-0442(2002)015⟨2907:ASMOAC⟩2.0.CO;2

Chun, J.-Y., Wood, R., Blossey, P., & Doherty, S. J. (2023). Microphysical, macrophysical, and radiative responses of subtropical marine clouds to aerosol injections. *Atmospheric Chemistry and Physics*, *23*(2), 1345–1368. https://doi.org/10.5194/acp-23-1345-2023

Dagan, G. (2022). Sub-tropical aerosols enhance tropical cloudiness—A remote aerosol-cloud lifetime effect. *Journal of Advances in Modeling Earth Systems*, *14*(12), e2022MS003368. https://doi.org/10.1029/2022MS003368

Dagan, G. (2024). Large-scale tropical circulation intensification by aerosol effects on clouds. *Geophysical Research Letters*, *51*(7), e2024GL109015. https://doi.org/10.1029/2024GL109015

Dagan, G., & Chemke, R. (2016). The effect of subtropical aerosol loading on equatorial precipitation. *Geophysical Research Letters*, *43*(20), 11048–11056. https://doi.org/10.1002/2016GL071206

Dagan, G., van den Heever, S. C., Stier, P., Abbott, T. H., Barthlott, C., Chaboureau, J.-P., et al. (2025). RCEMIP-ACI: Aerosol-cloud interactions in a multimodel ensemble of radiative-convective equilibrium simulations. *Journal of Advances in Modeling Earth Systems*, *17*(11), e2025MS005141. https://doi.org/10.1029/2025MS005141

Dagan, G., Yeheskel, N., & Williams, A. I. L. (2023). Radiative forcing from aerosol–cloud interactions enhanced by large-scale circulation adjustments. *Nature Geoscience*, *16*(12), 1092–1098. https://doi.org/10.1038/s41561-023-01319-8

Daniau, A.-L., Bartlein, P. J., Harrison, S. P., Prentice, I. C., Brewer, S., Friedlingstein, P., et al. (2012). Predictability of biomass burning in response to climate changes. *Global Biogeochemical Cycles*, *26*(4). https://doi.org/10.1029/2011GB004249

Deser, C., Phillips, A. S., Simpson, I. R., Rosenbloom, N., Coleman, D., Lehner, F., et al. (2020). Isolating the evolving contributions of anthropogenic aerosols and greenhouse gases: A new CESM1 large ensemble community resource. *Journal of Climate*, *33*(18), 7835–7858. https://doi.org/10.1175/JCLI-D-20-0123.1

Emanuel, K., Neelin, J. D., & Bretherton, C. S. (1994). On large-scale circulations in convecting atmospheres. *Quarterly Journal of the Royal Meteorological Society*, *120*(519), 1111–1143. https://doi.org/10.1002/qj.49712051902

Fan, J., Rosenfeld, D., Zhang, Y., Giangrande, S. E., Li, Z., Machado, L. A. T., et al. (2018). Substantial convection and precipitation enhancements by ultrafine aerosol particles. *Science*, *359*(6374), 411–418. https://doi.org/10.1126/science.aan8461

Gunn, R., & Phillips, B. B. (1957). AN experimental investigation of the effect of air pollution on the initiation of rain. *Journal of the Atmospheric Sciences*, *14*(3), 272–280. https://doi.org/10.1175/1520-0469(1957)014<0272:aeiote>2.0.co;2

Hartmann, D. L., & Michelsen, M. L. (1993). Large-scale effects on the regulation of tropical sea surface temperature. *Journal of Climate*, *6*(11), 2049–2062. https://doi.org/10.1175/1520-0442(1993)006<2049:lseotr>2.0.co;2

He, J., Lu, K., Fosu, B., & Fueglistaler, S. A. (2024). Diverging hydrological sensitivity among tropical basins. *Nature Climate Change*, *14*(6), 623–628. https://doi.org/10.1038/s41558-024-01982-8

Heede, U. K., & Fedorov, A. V. (2021). Eastern equatorial Pacific warming delayed by aerosols and thermostat response to CO2 increase. *Nature Climate Change*, *11*(8), 696–703. https://doi.org/10.1038/s41558-021-01101-x

Heever, S. C. v. d., Stephens, G. L., & Wood, N. B. (2011). Aerosol indirect effects on tropical convection characteristics under conditions of radiative–convective equilibrium. *Journal of the Atmospheric Sciences*, *68*(4), 699–718. https://doi.org/10.1175/2010JAS3603.1

Held, I. M., Hemler, R. S., & Ramaswamy, V. (1993). Radiative-convective equilibrium with explicit two-dimensional moist convection. *Journal of the Atmospheric Sciences*, *50*(23), 3909–3927. https://doi.org/10.1175/1520-0469(1993)050⟨3909:RCEWET⟩2.0.CO;2

Held, I. M., & Soden, B. J. (2006). Robust responses of the hydrological cycle to global warming. *Journal of Climate*, *19*(21), 5686–5699. https://doi.org/10.1175/JCLI3990.1

Hwang, Y.-T., Xie, S.-P., Chen, P.-J., Tseng, H.-Y., & Deser, C. (2024). Contribution of anthropogenic aerosols to persistent La Niña-like conditions in the early 21st century. *Proceedings of the National Academy of Sciences*, *121*(5), e2315124121. https://doi.org/10.1073/pnas.2315124121

Igel, A. L., & van den Heever, S. C. (2021). Invigoration or enervation of convective clouds by aerosols? *Geophysical Research Letters*, *48*(16), e2021GL093804. https://doi.org/10.1029/2021GL093804

Jeevanjee, N. (2022). Three rules for the decrease of tropical convection with global warming. *Journal of Advances in Modeling Earth Systems*, *14*(11), e2022MS003285. https://doi.org/10.1029/2022MS003285

Khairoutdinov, M. F., & Randall, D. A. (2003). Cloud resolving modeling of the ARM summer 1997 IOP: Model formulation, results, uncertainties, and sensitivities. *Journal of the Atmospheric Sciences*, *60*(4), 607–625. https://doi.org/10.1175/1520-0469(2003)060⟨0607:CRMOTA⟩2.0.CO;2

Latham, J. (1990). Control of global warming? *Nature*, *347*(6291), 339–340. https://doi.org/10.1038/347339b0

Li, R. L., Studholme, J. H. P., Fedorov, A. V., & Storelvmo, T. (2022). Precipitation efficiency constraint on climate change. *Nature Climate Change*, *12*(7), 642–648. https://doi.org/10.1038/s41558-022-01400-x

Lindzen, R. S., & Nigam, S. (1987). On the role of sea surface temperature gradients in forcing low-level winds and convergence in the tropics. *Journal of the Atmospheric Sciences*, *44*(17). https://doi.org/10.1175/1520-0469(1987)044⟨2418:otross⟩2.0.co;2

Mandorli, G., & Stubenrauch, C. J. (2024). Assessment of object-based indices to identify convective organization. *Geoscientific Model Development*, *17*(21), 7795–7813. https://doi.org/10.5194/gmd-17-7795-2024

McFarquhar, G. M., & Wang, H. (2006). Effects of aerosols on trade wind cumuli over the Indian Ocean: Model simulations. *Quarterly Journal of the Royal Meteorological Society*, *132*(616), 821–843. https://doi.org/10.1256/qj.04.179

Morrison, H., Curry, J. A., & Khvorostyanov, V. I. (2005). A new double-moment microphysics parameterization for application in cloud and climate models. Part I: Description. *Journal of the Atmospheric Sciences*, *62*(6), 1665–1677. https://doi.org/10.1175/JAS3446.1

Nishant, N., Sherwood, S. C., & Geoffroy, O. (2019). Aerosol-induced modification of organised convection and top-of-atmosphere radiation. *npj Climate and Atmospheric Science*, *2*(1), 33. https://doi.org/10.1038/s41612-019-0089-1

Pendergrass, A. G., & Hartmann, D. L. (2014). The atmospheric energy constraint on global-mean precipitation change. *Journal of Climate*, *27*(2), 757–768. https://doi.org/10.1175/JCLI-D-13-00163.1

Peters, M. E., & Bretherton, C. S. (2005). A simplified model of the walker circulation with an interactive ocean mixed layer and cloud-radiative feedbacks. *Journal of Climate*, *18*(20), 4216–4234. https://doi.org/10.1175/JCLI3534.1

Pierrehumbert, R. T. (1995). Thermostats, radiator fins, and the local runaway greenhouse. *Journal of the Atmospheric Sciences*, *52*(10), 1784–1806. https://doi.org/10.1175/1520-0469(1995)052⟨1784:TRFATL⟩2.0.CO;2

Pincus, R., & Baker, M. B. (1994). Effect of precipitation on the albedo susceptibility of clouds in the marine boundary layer. *Nature*, *372*(6503), 250–252. https://doi.org/10.1038/372250a0

Rosenfeld, D. (1999). TRMM observed first direct evidence of smoke from forest fires inhibiting rainfall. *Geophysical Research Letters*, *26*(20), 3105–3108. https://doi.org/10.1029/1999GL006066

Seifert, A., Heus, T., Pincus, R., & Stevens, B. (2015). Large-eddy simulation of the transient and near-equilibrium behavior of precipitating shallow convection. *Journal of Advances in Modeling Earth Systems*, *7*(4), 1918–1937. https://doi.org/10.1002/2015MS000489

Sobel, A. H., Nilsson, J., & Polvani, L. M. (2001). The weak temperature gradient approximation and balanced tropical moisture waves. *Journal of the Atmospheric Sciences*, *58*(23), 3650–3665. https://doi.org/10.1175/1520-0469(2001)058⟨3650:TWTGAA⟩2.0.CO;2

Sokol, A. B., & Hartmann, D. L. (2022). Congestus mode invigoration by convective aggregation in simulations of radiative-convective equilibrium. *Journal of Advances in Modeling Earth Systems*, *14*(7), e2022MS003045. https://doi.org/10.1029/2022MS003045

Sokol, A. B., Munteanu, V. A., Blossey, P. N., & Hartmann, D. L. (2025). Internal ocean-atmosphere variability in kilometer-scale radiative-convective equilibrium. *Journal of Advances in Modeling Earth Systems*, *17*(6), e2024MS004567. https://doi.org/10.1029/2024MS004567

Sokol, A. B., & Wright, C. J. (2026). Model output and code for sokol & wright (2026) [collection]. *Zenodo*. https://doi.org/10.5281/zenodo.19139137

Stevens, B., Cotton, W. R., Feingold, G., & Moeng, C.-H. (1998). Large-eddy simulations of strongly precipitating, shallow, stratocumulus-topped boundary layers. *Journal of the Atmospheric Sciences*, *55*(24), 3616–3638. https://doi.org/10.1175/1520-0469(1998)055<3616:lesosp>2.0.co;2

Takahashi, C., & Watanabe, M. (2016). Pacific trade winds accelerated by aerosol forcing over the past two decades. *Nature Climate Change*, *6*(8), 768–772. https://doi.org/10.1038/nclimate2996

Thornton, J. A., Virts, K. S., Holzworth, R. H., & Mitchell, T. P. (2017). Lightning enhancement over major oceanic shipping lanes. *Geophysical Research Letters*, *44*(17), 9102–9111. https://doi.org/10.1002/2017GL074982

Twomey, S. (1959). The nuclei of natural cloud formation part II: The supersaturation in natural clouds and the variation of cloud droplet concentration. *Geofisica pura e applicata*, *43*(1), 243–249. https://doi.org/10.1007/BF01993560

Twomey, S. (1974). Pollution and the planetary albedo. *Atmospheric Environment*, *8*(12), 1251–1256. https://doi.org/10.1016/0004-6981(74)90004-3

Williams, A. I. L., & Jeevanjee, N. (2025). A robust constraint on the response of convective mass fluxes to warming. *Journal of Advances in Modeling Earth Systems*, *17*(4), e2024MS004695. https://doi.org/10.1029/2024MS004695

Williams, I. N., & Pierrehumbert, R. T. (2017). Observational evidence against strongly stabilizing tropical cloud feedbacks. *Geophysical Research Letters*, *44*(3), 1503–1510. https://doi.org/10.1002/2016GL072202

Wing, A. A., Emanuel, K., Holloway, C. E., & Muller, C. (2017). Convective self-aggregation in numerical simulations: A review. *Surveys in Geophysics*, *38*(6), 1173–1197. https://doi.org/10.1007/s1071201794084

Wing, A. A., Reed, K. A., Satoh, M., Stevens, B., Bony, S., & Ohno, T. (2018). Radiative–convective equilibrium model intercomparison project. *Geoscientific Model Development*, *11*(2), 793–813. https://doi.org/10.5194/gmd-11-793-2018

Wing, A. A., Stauffer, C. L., Becker, T., Reed, K. A., Ahn, M.-S., Arnold, N. P., et al. (2020). Clouds and convective self-aggregation in a multimodel ensemble of radiative-convective equilibrium simulations. *Journal of Advances in Modeling Earth Systems*, *12*(9), e2020MS002138. https://doi.org/10.1029/2020MS002138

Wood, R. (2007). Cancellation of aerosol indirect effects in marine stratocumulus through cloud thinning. *Journal of the Atmospheric Sciences*, *64*(7), 2657–2669. https://doi.org/10.1175/JAS3942.1

Wright, C. J., Thornton, J. A., Jaeglé, L., Cao, Y., Zhu, Y., Liu, J., et al. (2025). Lightning declines over shipping lanes following regulation of fuel sulfur emissions. *Atmospheric Chemistry and Physics*, *25*(5), 2937–2946. https://doi.org/10.5194/acp-25-2937-2025

Xing, C., Stevenson, S., Fasullo, J., Harrison, C., Chen, C., Wan, J., et al. (2025). Subtropical marine cloud brightening suppresses the El niño–southern oscillation. *Earth's Future*, *13*(8), e2025EF006522. https://doi.org/10.1029/2025EF006522

Yamaguchi, T., Yoshida, R., Chen, Y.-S., McCoy, I. L., & Feingold, G. (2026). Dynamical and radiative influence on the hadley circulation by aerosol-cloud interactions. *Journal of Advances in Modeling Earth Systems*, *18*(4), e2025MS005465. https://doi.org/10.1029/2025MS005465

References From the Supporting Information

Mlawer, E. J., Taubman, S. J., Brown, P. D., Iacono, M. J., & Clough, S. A. (1997). Radiative transfer for inhomogeneous atmospheres: RRTM, a validated correlated-k model for the longwave. *Journal of Geophysical Research*, *102*(D14), 16663–16682. https://doi.org/10.1029/97JD00237

Yamaguchi, T., Randall, D. A., & Khairoutdinov, M. F. (2011). Cloud modeling tests of the ULTIMATE–MACHO scalar advection scheme. *Monthly Weather Review*, *139*(10), 3248–3264. https://doi.org/10.1175/MWR-D-10-05044.1